ASSESSMENT OF HEAVY METAL CONTAMINANTS IN GROUNDWATER AROUND MINING AREA BY USING METAL POLLUTION INDICES MULTIVARIATE ANALYSIS AND GIS TECHNIQUE

Vijayendra Pratap Dheeraj[1], Chandra Shekhar Singh[1], Ashwani Kumar Sonkar[1], Saurabh Kumar Barman[2]

[1]Department of Mining Engineering, Indian Institute of Technology (Banaras Hindu University), Varanasi 221005, India
[2]Department of Geology, Centre of Advance Studies Institute of Science (Banaras Hindu University), Varanasi 221005, India
E-mail: vijayendrapdheeraj.rs.min19@itbhu.ac.in

Received 13 July 2023
Accepted 07 October 2023
DOI: 10.59957/jctm.v59.i4.2024.20

ABSTRACT

An opencast and underground coal mining each have the potential to have a negative impact on the groundwater table in terms of both its quantity and quality. Leachates from overburden dumps and industrial waste are another issue worldwide; they infiltrate into the groundwater and have a negative impact on the quality of it. A concern is that groundwater will become contaminated with heavy metals. Therefore, in the current study, the groundwater sample have been collected systematically from different sources of water in pre monsoon season (May) of 2022 around Korba coalfield (KCF). The collected water samples were examined for 9 different heavy metals by using ICP-MS (Inductively Coupled Plasma Mass Spectrometer-Perkin Elmer, Optima 4300 DV) instrument. In general, the concentrations of few metals such as Aluminium, Cadmium, Copper, Iron, Lead, and Zinc were found to be well below the acceptable limits of World Health Organization (WHO) and Bureau of Indian Standards (BIS) standard, however Manganese, Barium, and Nickel concentrations were observed to be above to desirable limits of WHO and BIS standard at a few sites which is similar to the results obtained by previous studies. These laboratory data were applied for the calculation of heavy metal pollution indices such as Heavy Metal Pollution Index (HPI), Heavy Metal Evaluation Index (HEI), and Contamination Index (Cd). The multiple approach used to evaluate the metal indices identifies that 80 % of HPI, 85 % of HEI, and 95 % of Cd for groundwater samples mostly classified as "low to medium" class. The spatial diagram of these different indices showed a higher value in the south east part of the region suggesting that the heavy metal leaching from mining activities has little impact on the groundwater in the south east of the examined area. Multivariate statistical studies, like principal component analysis (PCA) analysis reveals that Fe, Pb, and Zn originate from anthropogenic sources like coal mining, while Al and Cd originate from both lithogenic and anthropogenic sources.

Keywords: groundwater, heavy metals, pollution indices, spatial distribution map.

INTRODUCTION

Fossil fuel like coal has become an essential source worldwide in generating electricity [1]. Coal is the second most essential source of energy, accounting for an estimated 29.20 % of world energy consumption. Coal demand is anticipated to be around 7700 million tonnes (MT) globally [2]. India is the third-largest coal producer in the world, producing 638 MT (2015 - 2016), generating more than 70 % of the nation's electricity, as per Ministry of Coal 2016 statistics. The demand for portable water has been sharply enhanced due to the increase in population as well as surface water scarcity around some parts of the world. Groundwater is one of the most easily available and accessible raw materials, with extraction rates as high as 982 km^2 $year^{-1}$ [3 - 7]. The few available trace elements in groundwater like Fe, Zn, Mn, Cu, and Ni are important in less quantities but it is very toxic at a higher concentration for human, plant growth, and animal metabolism [8] meantime some others elements like Cd and Pb are highly toxic even at relatively less concentration [8, 9]. As per United Nations Environment Programme report (2000), a few anthropogenic activities like mining for minerals, the discharge of untreated and semi-treated metal industry effluents, sewage disposal, manufacturing industries, and the use of agrochemicals in agriculture are the primary causes of toxic trace elements in nearby groundwater bodies. Additionally, the toxic metals into their surroundings by dispersion of fly ash and leachates from pond ash released from a thermal power plant with the process of coal combustion and fusion [7, 9].

Toxic metals cannot be destroyed by biological processes; therefore, they may survive in the body and harm internal organs as well as the neurological system [10, 11]. In India, approx. 21 % of communicable diseases are essentially water-borne [12]. Therefore, this study is an effort made to bring social benefits to the individuals living in this region. Only a few studies have been performed to examine the extent of heavy metal contamination in the groundwater around the Korba Coalfield [13 - 15]. Thus, the present study was carried out in Korba coalfields region, India, with the intention of examining the potential adverse effects of coal mining operations on groundwater quality. The different water pollution indices were applied to assess the overall impact of heavy metals in groundwater. Whereas spatial distribution map, correlation matrix and PCA analysis has been used for source identification.

EXPERIMENTAL

Study area

The study area is located in Korba district Chhattisgarh, India. The total study area is covered around 226.57 km^2 which lies the between latitude of 22°16’44.4”N and 22°22’51.6”N and Longitude 82°28’26.4”E and 82°42’57.6”E (Fig. 1). The selected region is covered by Survey of India (SOI) Toposheet no. F44K11. It is the largest coal mine in India, and its three mega projects are Gevra open cost, Dipka open cost, and Kushmunda open cost. Additionally, the Chhattisgarh State Electricity Board (CSEB) and the National Thermal Power Plant (NTPC) both have their headquarters in this region. The soil exist in this region is sandy loom (Lf - 3791) as per UNESCO. The average rainfall in this district was recorded at about 1506 mm with 1287 mm in the monsoon season. The region is dominated both by agriculture and by barren land, which together accounts for around 54 % of the total selected area. The geomorphology of the area includes the pediment Pedi plain complex, low dissert hills and valleys, quarry and mine dump, and water bodies [16, 17].

The KCF formations are part of the Permo-Carboniferous Gondwana Supergroup, which also includes the Barakar, Talchir, and Kamthi Formations, and are underlain by the Precambrian Schist [18]. The area is identified by upper member of the Early Permian Barakar Formation, which belongs to the Lower Gondwana Group and trends E-W with a general dip of 5°-8° to the south. This region has a large number of transverse faults with varied throw magnitudes that trend NE-SW, NW-SE, and E-W, giving it its particular structural features [19].

The area features a multiple layer aquifer system caused by the stratification of diverse lithological units such as coal distribution, and carbonaceous shale strata between sandstone layers, combined with the shale and sandstone strata of different grain sizes. Aquicludes are shale beds and coal seams with limited transmissivity, whereas aquifers are saturated sandstone beds with a porous character and the appropriate transmissivity. The water table has a gradient of 1.2×10^{-3} that slopes towards the south or south east and is essentially horizontal in the area.

Data collections and its analysis

In this study, twenty groundwater samples have been collected in pre monsoon season of 2022 to determine the groundwater purity with respect to heavy metals by using different indices like HPI, HEI, and Cd. The water samples are taken from all possible sources such as hand pump, dug well and bore well from the surrounding area of KCF region, Chhattisgarh as shown in Fig. 2. The polyethylene bottle having a capacity of 100 mL were used for the samples collection. The collected groundwater samples were filtered with 0.22 µm syringe filter. The polyethylene bottles are washed twice through the ultrapure water to avoid any contamination and each sample has been acidified with nitric acid (pH < 2) and stored at 4^{o}C until analysis.

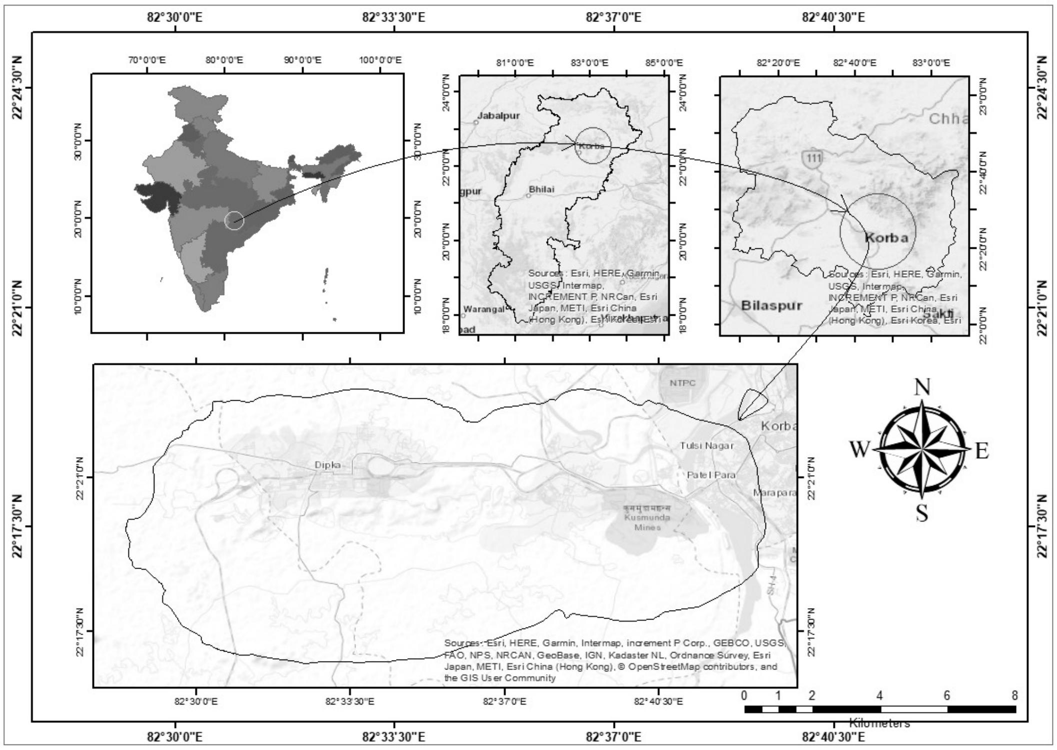

Fig. 1. Study area map of KCF region.

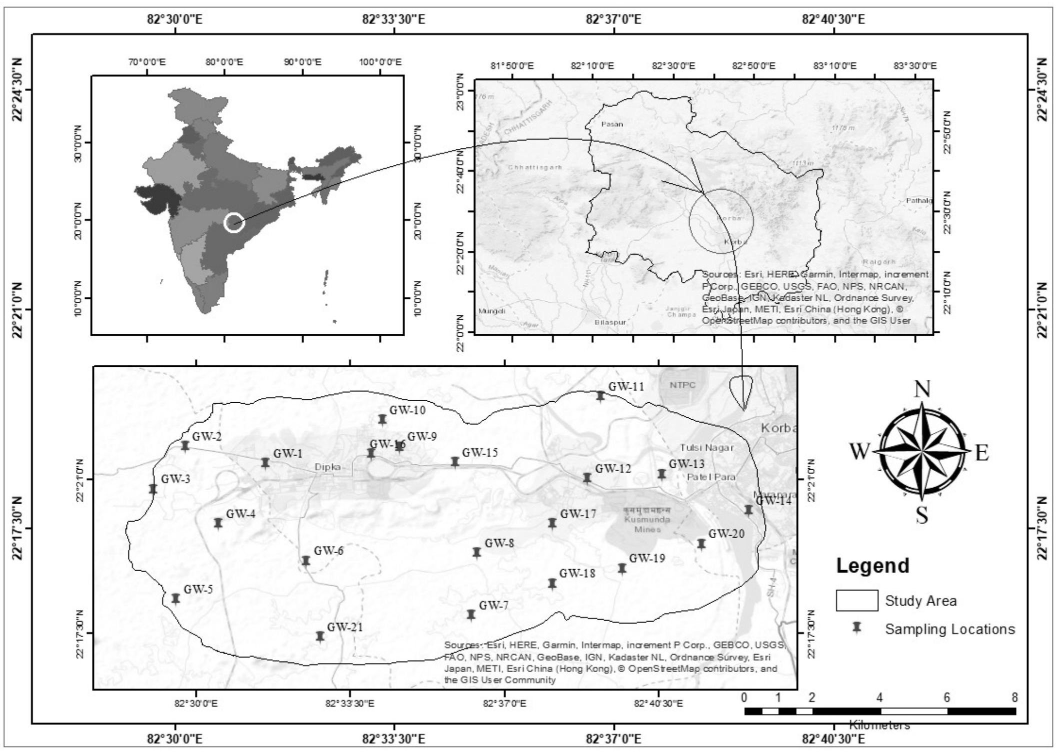

Fig. 2. Sampling map of the study area.

ICP - MS has been employed for determine the concentration of the metals in groundwater [20].

Only Milli-Q water, which is ultra-pure water, used for the entire analysis of heavy metals. Analytical grade solutions were employed to clean the glassware. To begin, blank reagent is used to verify ICP - MS results. For each of the ten samples, a calibration blank and an independent calibration verification standard were checked to confirm the calibration status of the ICM-MS. Matrix interference is present in < 1 % of all elements (blank). The degree of precision achieved in this study was more than 5 % RSD in all instances with a corresponding precision.

Metal indices analysis

Metals indices such as HPI, HEI and Cd were used to examine the suitability of groundwater for drinking and domestic usage by comparing with WHO and BIS [21, 22]. The estimated HPI and HEI show the overall water quality in terms of heavy metals, whereas Cd reflects the combined effects of a number of quality parameters considered to be unhealthy in drinking water. These pollution evaluation indices are very helpful in describing as well as quantifying the water quality trends regarding heavy metals present in water.

Heavy metal pollution index

The HPI is a rating system that determines the overall effect of individual metals on water quality based on empirical evidence. The grading system gives an approximate sense of an arbitrary number that varies from 0 to 1, based on the importance of each parameter on overall quality. The Unit weightage (W_i) of relative parameters employed in HPI computation is inversely proportional to standard value (S_i). The critical HPI value for drinking water is 100 [23].

B. Prasad, J. Bose have estimated HPI by the relationship as given below [23].

$$HPI = \frac{\sum_{i=1}^{n} WiQi}{\sum_{i=1}^{n} Wi} \quad (1)$$

where W_i - unit weight of i^{th} variables, n - Number of parameters and Q_i - Sub-index of i^{th} variables computed.

$$Qi = \sum_{i=1}^{n} \frac{(Mi(-)Ii)}{(Si - Ii)} \times 100 \quad (2)$$

where M_i - Analytical data, I_i - Ideal value, S_i - Standard value and (-) - represents a numerical difference between value.

Heavy metal evaluation index

A.E Edet, O.E Offiong described that HEI provides the overall water quality in reference to heavy metals just like the HPI index [24]. It is also utilized for easy interpretation of the pollution level of heavy metals in water samples [25]. HEI can be determine as given under.

$$HEI = \sum_{i=1}^{n} \frac{Mi}{Si} \quad (3)$$

where M_i - Monitored value, S_i - Standard permissible values and n - Number of parameters

Contamination index

The Water quality is evaluated or estimated through the contamination index (Cd) calculation. Backman et al. described that the complex impact of various parameters is considered very hazardous in domestic water [26]. The calculation of Cd is mentioned as under.

$$Cd = \sum_{i=1}^{n} Cfi \quad (4)$$

where $Cfi = \frac{CAi}{CNi} - 1$,

where C_{fi} - contamination factor, C_{Ai} - analytical value, C_{Ni} - maximum permissible values and N - normative value.

Multivariate statistical analysis

Multivariate statistical studies, such as principal component analysis (PCA) and correlation analysis are used for source identification. In this study, multivariate analyses were performed using Origin-Pro 2017 which was provided by the Centre for Computing and Information Services, IIT (BHU) Varanasi. PCA analysis is one of the most used statistical methods for reducing composite dataset into explanatory principal components (PCs). This enables the identification of crucial factors without affecting the information of the data [27]. This technique is used to quantify and clarify the interconnections between various factors [28]. Moreover, Microsoft Excel 2019 was used to calculate the correlation coefficient (r) between samples to determine metal associations.

RESULT AND DISCUSSION

The statistical summary of heavy metals concentration along with its confidence intervals are mentioned in Table 1 and Table 2. The concentrations of few metals like Al, Cd, Cu, and Zn were lower than the acceptable limits [21, 22]. Whereas Cd concentration range from 0.02 to 1.49 μg L^{-1} with an average value of 0.17 μg L^{-1} which is below the required limit of 3 μg L^{-1} [21]. Copper concentrations range from 0.0 to 50.71 μg L^{-1}, with an average value of 5.57 μg L^{-1} that does not exceed to permissible limit of 1500 μg L^{-1} [22]. The Zn concentration ranges from 0 to 11766.915 μg L^{-1} with a mean value of 825.56 μg L^{-1} which does not exceed the maximum permissible limit of 15000 μg L^{-1} [22] (Table 1). In a few locations, Mn, Ba, and Ni concentrations have been measured to be higher than the highest recommended limit [22]. The concentration of Mn ranges from 17.53 to 367.68 μg L^{-1} with an average value of 105.41 which exceeded the maximum permissible value of 300 μg L^{-1} at two sampling sites (GW-7 and GW-10).

The concentration of Ba ranges from 27.98 to 2457.22 μg L^{-1} with an average value of 15.95, exceeded the maximum desirable limit of 700 μg L^{-1} at two sample sites (GW-2 and GW-10). whereas Ni concentrations ranges from 0 to 69.87 μg L^{-1} with an average value of 15.13, exceeded the maximum allowable value of 20 μg L^{-1} at four sampling sites: GW-7, GW-8, GW-10 and GW-14 respectively [21]. Fe, and Pb concentrations have been found to exceed the desirable limit of drinking water standards in two different locations. The Fe concentrations exceeded the maximum desired value of 300 μg L^{-1} in GW-6. Whereas, the concentration of Pb exceeded the maximum desirable limit of 10 μg L^{-1} at GW-10 [21, 22].

Fe and Mn have a negligible influence on the HPI

Table 1. Summary statistic of various elements compared with [21, 22].

Metals	Minimum	Maximum	Mean	Std dev.	WHO (2006)	BIS 2012	
						Required	Per. limit
Al	0.00	176.57	15.95	39.13	100-200	30	200
Ba	27.98	2457.22	354.98	548.87	300	700	No relaxation
Cd	0.02	1.49	0.17	0.33	3	3	No relaxation
Cu	0.00	50.71	5.57	13.54	2000	50	1500
Fe	0.00	2892.06	175.99	644.08	300	300	No relaxation
Mn	17.53	367.68	105.41	102.62	100	100	300
Pb	0.00	67.37	3.92	14.98	10	10	No relaxation
Ni	0.00	69.87	15.13	21.94	20	20	No relaxation
Zn	0.00	11766.92	825.56	2703.02	4000	5000	15000

The units of variables in μg L^{-1}

Table 2. Confidence interval of average results obtained for the metals concentration.

Metals	Kurtosis	Skewness	Confidence Interval (90.0 %)	Confidence Interval (95.0 %)
Al	17.78	4.11	14.35	17.36
Ba	12.72	3.35	201.35	243.52
Cd	16.16	3.85	0.12	0.15
Cu	7.78	2.86	4.97	6.01
Fe	20.16	4.46	236.27	285.76
Mn	2.57	1.77	37.64	45.53
Pb	20.59	4.52	5.49	6.65
Ni	1.45	1.56	8.05	9.73
Zn	16.69	4.01	991.56	1199.25

value because they are given very small weightage (W_i). Few metals like Pb, and Cd have received no relaxation in drinking water standards and have high weightage (W_i) value in the HPI. As a result, even small concentrations of these pollutants in water samples lead to poor water quality and high HPI ratings. Overall, there isn't much of an issue with heavy metals contaminating the groundwater in the Korba Coalfield area except GW-10.

Evaluation of spatial distribution diagram

The spatial distribution map demonstrates the source identification in the area. The south-eastern, north region of the study area have higher levels of Mn concentration as shown in Fig. 3. whereas, the spatial distribution diagram of Ba concentration indicates that east and western side has high concentrations and the rest part shows the low concentration as well (Fig. 4). The spatial distribution diagram of Ni concentration shows the high concentration in the south-eastern and north side of the region as shown in Fig. 5. The other metals were well below the permissible limits.

Correlation Matrix

The correlation analysis of heavy metals has been presented in the study area as given in Table 3. It shows the degree of correlation and the correlation between variables based on the magnitude of Pearson's coefficient (r) of correlation. The positive correlation indicates that as one parameter rise, another parameter also rises in parallel with it. The negative correlation shows that, their sources as well as characteristics are not homogeneous and the value of one parameter increases while the other value decreases. The strong positive correlation between Fe - Pb (0.988), Fe - Zn (0.942), Pb - Zn (0.971), and Mn - Zn (0.685) has been established which indicating that their source is same. However, a negative correlation between Al - Mn (-0.199), Al - Cd (-0.169), and Al - Ni (-0.168) were found which indicates different sources of origin.

Estimations of metals pollution Indices

The HPI has been computed using the prescribed formula by Eq. 1. The value of HPI ranges between 0.61

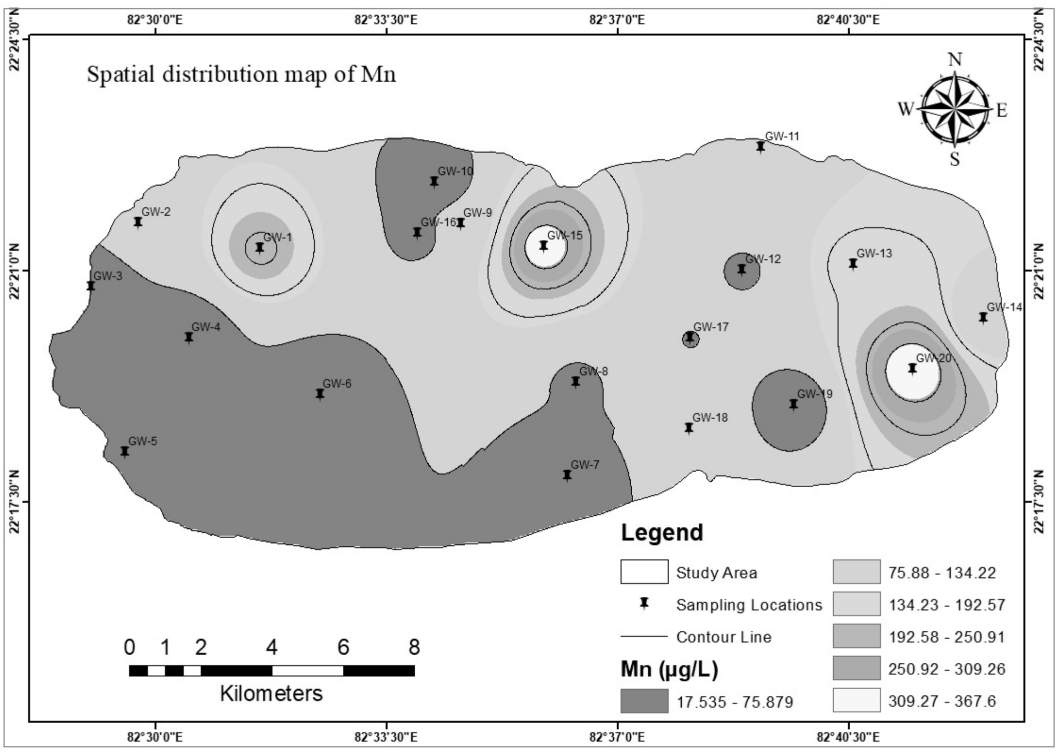

Fig. 3. Spatial diagram for Mn concentration.

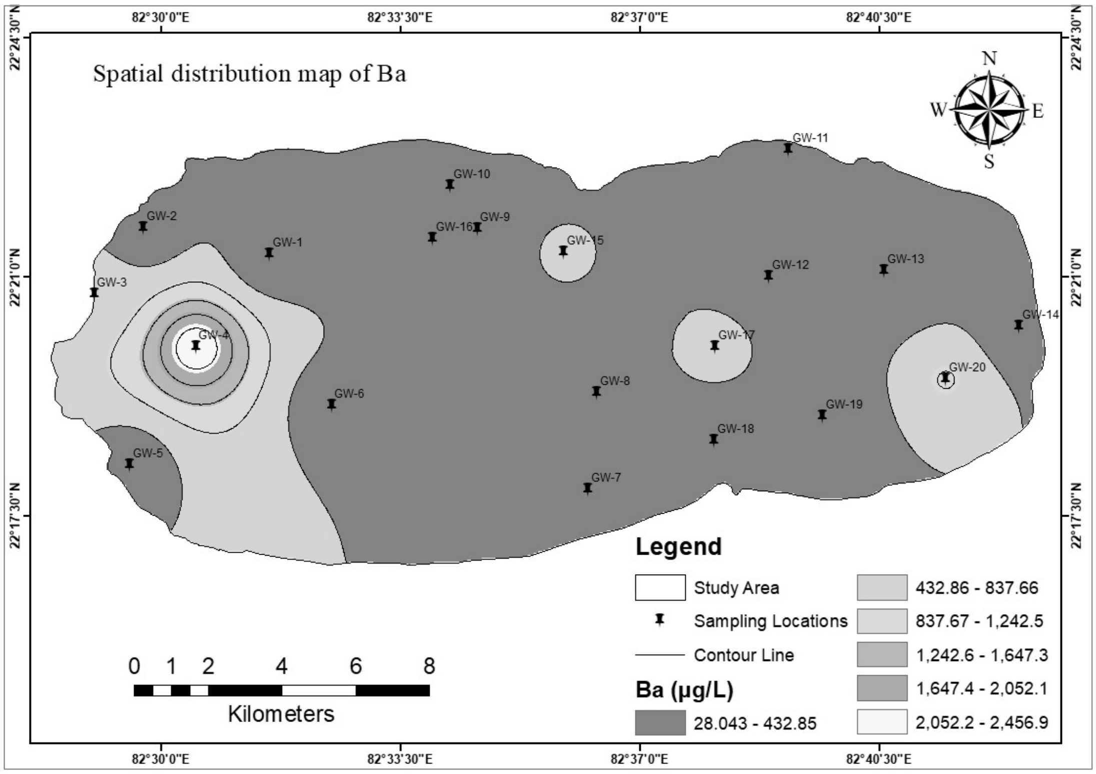

Fig. 4. Spatial diagram for Ba concentration.

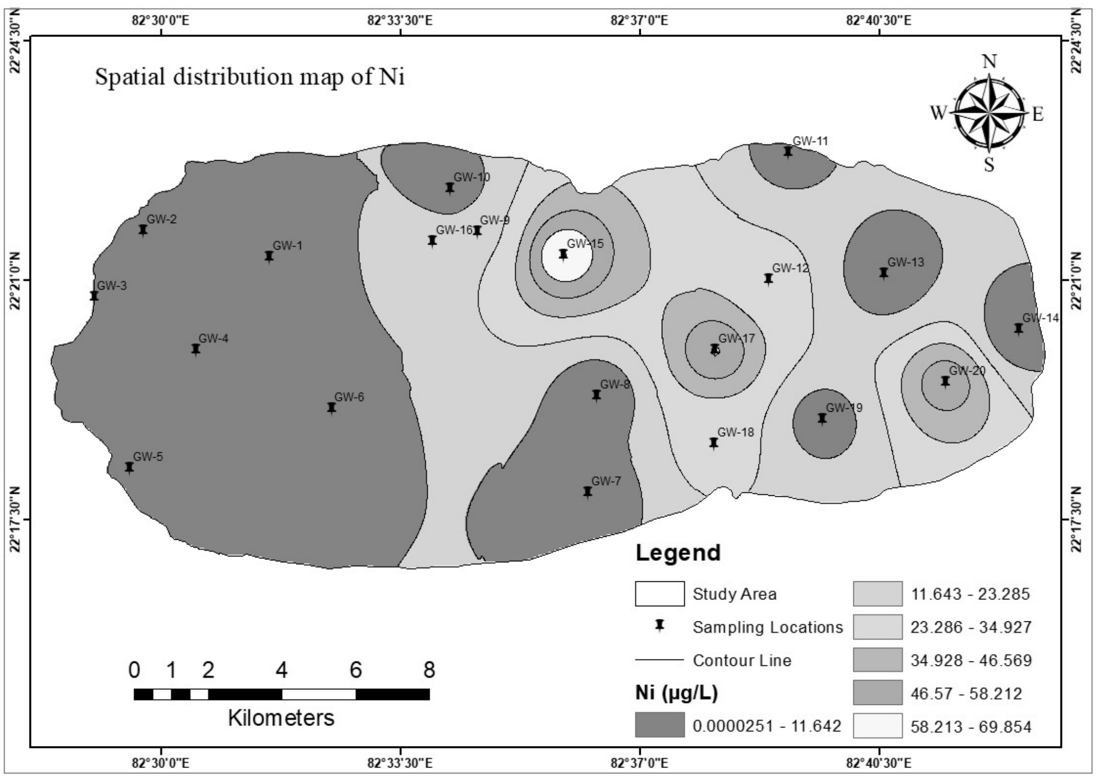

Fig. 5. Spatial diagram for Ni concentration.

to 169.88 as given in Table 4. It was found that 80 % of water samples (GW - 2, 3, 4, 5, 6, 7, 8, 9, 10, 11, 12, 13, 14, 16, 18, 19) comes under low pollution level and rest 20 % of water samples (GW - 1, 15, 17, 20) classified into high pollution level (Table 5). Whereas no any samples belong to medium pollution level of HPI. The higher value of HPI is 169.88 (GW - 20) calculated in the area. The spatial distribution diagram of HPI shows the high concentration in the south east side of the region as shown in Fig. 6. The area is minorly affected with heavy metal leaching from mining operation as well as transportation routes. The HPI is classified in three class as shown in Table 4 [24].

Moreover, another HEI ranges between 0.496 to 22.48 as given in Table 4. It was found that 70 % of water samples (GW - 2, 3, 5, 6, 7, 8, 10, 11, 12, 13, 14, 16, 19, 20) comes under low pollution level, 15 % of water samples (GW - 1, 4, 9) in medium level and rest 15 % (GW - 15, 17, 18) in high pollution level (Table 5). The high value of HEI is observed at GW-20 in east part of the region as shown in Fig. 7.

The contamination index (Cd) is also calculated to know the pollution level in the area. The calculated contamination index value ranges between -9.5 to 12.48 (Table 4). Three categories, low Cd < 1, medium 1 < Cd > 3, and Cd > 3 are used to categorise

Table 3. Correlation Matrix among the heavy metals (n = 20).

Metals	Al	Ba	Cd	Cu	Fe	Mn	Pb	Ni	Zn
Al	1	0.091	-0.169	-0.166	-0.115	-0.199	-0.104	-0.168	-0.129
Ba	0.091	1	-0.072	0.040	0.208	0.037	0.231	0.127	0.180
Cd	-0.169	-0.072	1	-0.081	0.055	0.438	0.140	0.100	0.356
Cu	-0.166	0.040	-0.081	1	0.631	0.419	0.524	0.065	0.494
Fe	-0.115	0.208	0.055	0.631	1	0.608	0.988	0.396	0.942
Mn	-0.199	0.037	0.438	0.419	0.608	1	0.634	0.636	0.685
Pb	-0.104	0.231	0.140	0.524	0.988	0.634	1	0.419	0.971
Ni	-0.168	0.127	0.100	0.065	0.396	0.636	0.419	1	0.379
Zn	-0.129	0.180	0.356	0.494	0.942	0.685	0.971	0.379	1

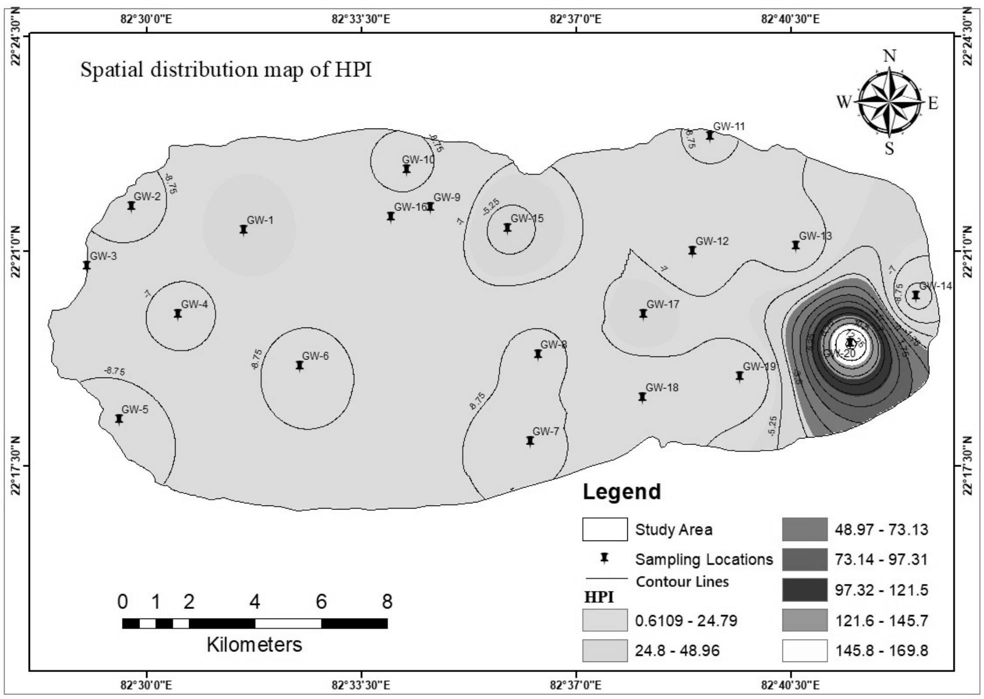

Fig. 6. Spatial diagram for HPI.

Table 4. Site details with calculated water pollution indices.

S No.	Latitude (N)	Longitude (E)	Source of water	HPI	HEI	Cd
	22.355514	82.526496	GW-1	43.42	2.28	-7.13
	22.361964	82.495823	GW-2	1.95	0.69	-9.31
	22.345766	82.483843	GW-3	1.46	1.27	-8.73
	22.33275	82.508577	GW-4	4.73	3.93	-6.07
	22.304122	82.4925489	GW-5	3.82	0.59	-9.41
	22.318646	82.541605	GW-6	7.91	0.69	-9.31
	22.298111	82.604188	GW-7	3.14	0.56	-9.44
	22.321711	82.606275	GW-8	0.61	0.73	-9.28
	22.361737	82.577107	GW-9	12.19	2.00	-8.01
	22.372027	82.570585	GW-10	2.05	0.50	-9.5
	22.380998	82.653004	GW-11	3.81	0.76	-9.24
	22.349923	82.648221	GW-12	7.82	1.91	-8.09
	22.351409	82.676303	GW-13	1.57	1.85	-8.15
	22.337723	82.709064	GW-14	3.38	0.70	-9.3
	22.356015	82.598106	GW-15	43.79	5.72	-4.28
	22.359209	82.566359	GW-16	12.38	1.61	-8.39
	22.332723	82.635027	GW-17	33.71	4.21	-5.78
	22.310044	82.634805	GW-18	13.91	1.90	-8.1
	22.315807	82.661151	GW-19	3.28	1.39	-8.61
	22.324969	82.691156	GW-20	169.9	22.48	12.48
Mean				18.741	2.788	-7.183
Min				0.61	0.496	-9.5
Max				169.88	22.48	12.48

GW - Groundwater

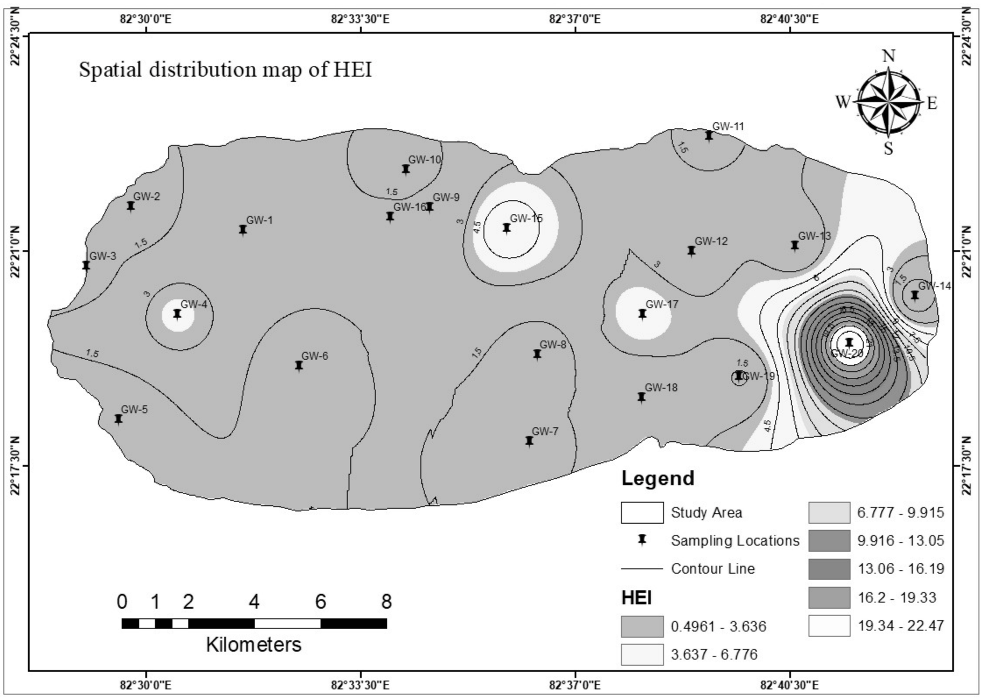

Fig. 7. Spatial diagram for HEI.

the contamination index [26]. It has been found that 95 % of water samples fall under the low pollution level and the rest 5 % are in a high pollution level as given in Table 5. Based on spatial distribution diagram, it was found that the east part of the area is affected with a high (Cd = 12.48) value as shown in Fig. 8.

The groundwater pollution indices for the area were 80 % of HPI, 85 % of HEI, and 95 % of Cd fall into "low to medium" category which are safe for drinking and domestic use. The pollution indices in the pre-monsoon season were reported to be 100 %, 94 %, and 87 % in a previous study for the same work from 2017 [29].

This suggests that over several years, the groundwater in the mining area seems to have become minorly affected with heavy metals at few locations in the selected area. The groundwater was not more contaminated with metal concentration as per the determined metal indices value.

Table 5. Water quality classification according to pollution indices categories.

Indices methods	Category	Degree of pollution	Number of samples	Percentage (%)	Samples
Heavy metal pollution index	< 15	Low	16	80	GW - 2, 3, 4, 5, 6, 7, 8, 9, 10, 11, 12, 13, 14, 16, 18, 19
	15 - 30	Medium	0	0	Nil
	> 30	High	4	20	GW - 1, 15, 17, 20
Heavy metal evaluation index	< 2	Low	14	70	GW - 2, 3, 5, 6, 7, 8, 10, 11, 12, 13, 14, 16, 19, 20
	2 - 4	Medium	3	15	GW - 1, 4, 9
	> 4	High	3	15	GW - 15, 17, 18
Contamination index	< 0.5	Low	19	95	GW - 1, 2, 3, 4, 5, 6, 8, 9, 10, 11, 12, 13, 14, 16, 17, 18, 19, 20
	0.5 - 1	Medium	0	0	Nil
	> 1	High	1	5	GW - 7

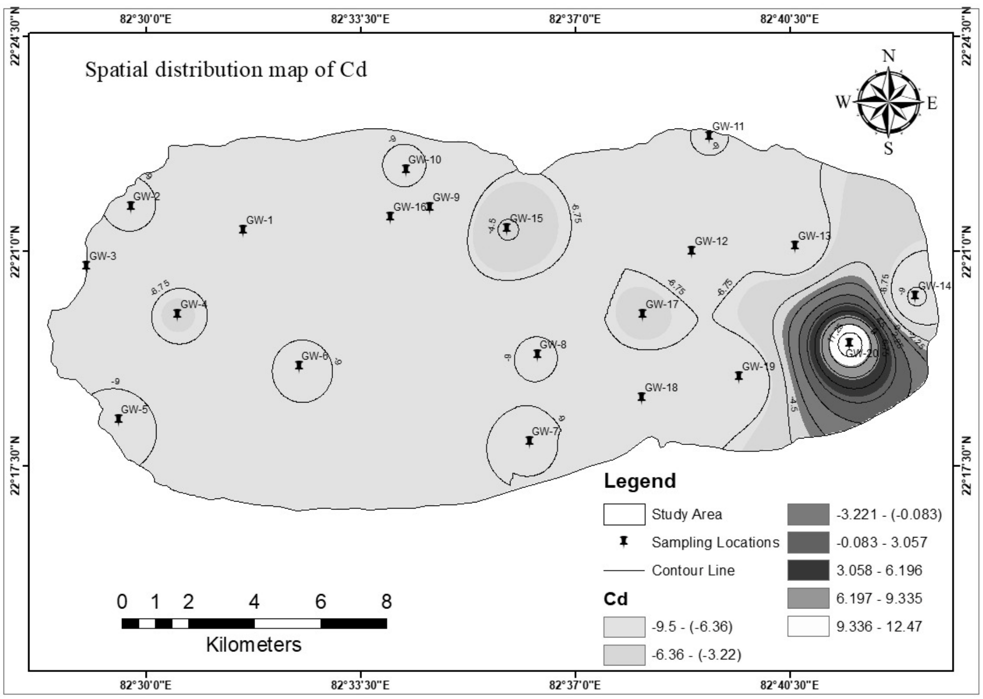

Fig. 8. Spatial diagram for Cd.

Source identification based on PCs analysis

Typically, eigenvalues are utilized in the PCA analysis approach for identifying the primary components. It reduces the total number of variables used in statistical assessments of the area. Scree plot (Fig. 9) of PCA analysis is derived based on eigenvalues (> 1) for the complete dataset along with 9 heavy metals. PCA analysis has been performed to assess the extent of metals pollution and source identification through standard procedure as reported in the different literature [30 - 33]. The loadings of measured metal concentrations in the coordinate system of three main components (PC) are generated by considering the correlation matrix. For inter-element correlations, factor loadings (> 0.75) were considered "high", (between 0.50 and 0.75) "moderate", and (< 0.5) "low" [34].

PC1 is the most significant factor as it accounts for 46.70 % of the variance and has low positive loadings of Fe, Pb, and Zn (< 0.459) as given in Table 6. PC1 can be identified as an anthropogenic source, specifically the effluents from coal mines. The galena (PbS) and

Table 6. PCs Loadings, varimax, eigenvalues for metals concentration in groundwater.

Metals	PC1	PC2	PC3
Al	-0.109	0.401	0.424
Ba	0.102	0.385	0.591
Cd	0.138	-0.623	0.185
Cu	0.298	0.273	-0.519
Fe	0.459	0.227	-0.089
Mn	0.397	-0.304	0.103
Pb	0.462	0.167	0.008
Ni	0.271	-0.235	0.385
Zn	0.463	0.026	0.016
Eigenvalue	4.203	1.368	1.073
% of Variance	46.70 %	15.20 %	11.92 %
Cumulative	46.70 %	61.90 %	73.82 %

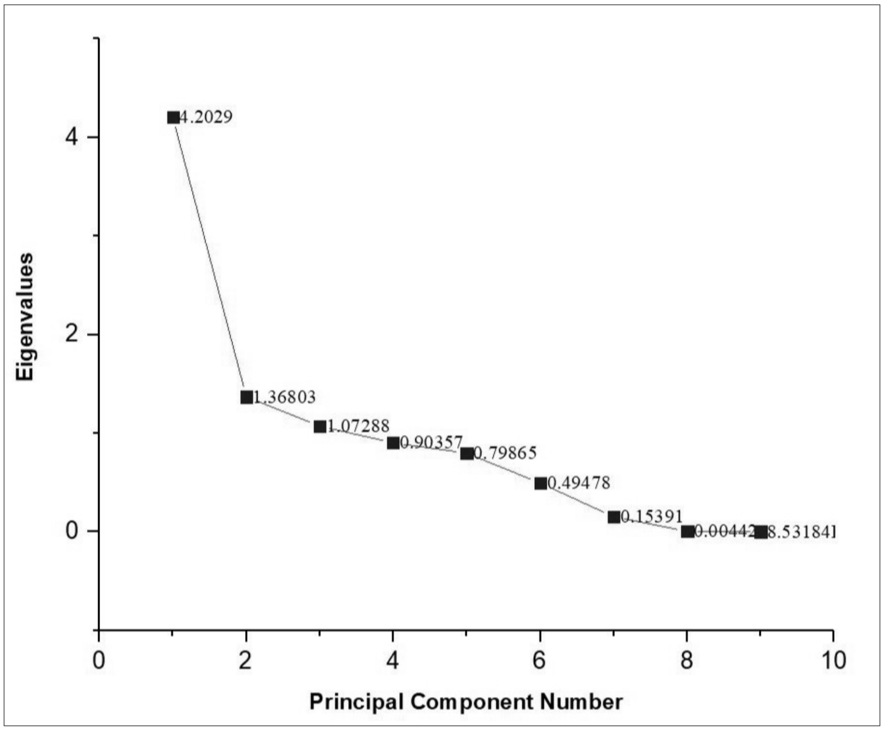

Fig. 9. PCA Scree plot for eigenvalue of nine metals.

sphalerite (ZnS) minerals that are typically found in association with coal seams have the potential to release Pb and Zn. Other studies have shown comparable results [30, 31]. PC2 is responsible for 15.20 % of the variation in the data, and it exhibits low positive loadings of Al (+0.401) and low negative loadings of Cd (-0.623). PC2 can be interpreted as a measure of lithogenic metals leaching from crustal minerals. whereas, PC3 represents 11.92 % of the variance with moderate positive loading of Al and Ba (< 0.591) and low negative loadings Cu (-0.519) which indicates mixed source lithogenic and anthropogenic contributions.

CONCLUSIONS

According to the findings, 80 % of HPI, 85 % of HEI, and 95 % of Cd predominantly lied under "low to medium" category of pollution demonstrating that the water is safe for drinking and for domestic purposes in pre monsoon season. In previous research from 2017 for the same work, it was reported that the indices for groundwater in the pre monsoon season were 100 %, 94 %, and 87 % [29]. Only one sample of this works exceeded the HPI critical level of 100. The spatial distribution of different indices provides good concordance with the spatial diagram of metals and demonstrate that these pollution indices have slightly more concentrated, notably in the eastern side of the area. it suggests that over a number of years, the groundwater in the mining area seems to have become minorly affected with respect to heavy metals. This study also used multivariate studies like PCs analysis as well as correlation matrix for the source identification. This sort of diligent study may assist planners and policymakers in the future in developing preventive measures against negative environmental impacts produced by mining operations through the deployment of appropriate mitigation solutions.

Acknowledgment

The authors thankfully acknowledge Indian Institute of Technology (Banaras Hindu University) for providing the financial support for the present study and management of Korba Coalfield for the support during the collections of the water samples.

REFERENCES

1. C. Belviso, F. Cavalcante, S.Di Gennaro, A. Palma, P. Ragone, S. Fiore, Mobility of trace elements in fly ash and in zeolitised coal fly ash, Fuel, 144, 2015, 369-379.
2. World Energy Council, World energy resource summary, 2016.
3. S. Shukla, A. Saxena, Sources and leaching of nitrate contamination in groundwater, Current Science, 118, 6, 2020, 883-891.
4. S. Shukla, A. Saxena, Water quality index assessment of groundwater in the Central Ganga Plain with reference to Raebareli district, Uttar Pradesh, India, Current Science, 119, 8, 2020, 1308-1315.
5. V.P. Dheeraj, C.S. Singh, N. Kishore, A.K. Sonkar, Groundwater Quality Assessment in Korba Coalfield Region, India: An Integrated Approach of GIS and Heavy Metal Pollution Index (HPI) Model, Nature Environment & Pollution Technology, 22, 1, 2023, 369-382.
6. D.P. Shukla, C.S. Dubey, N.P. Singh, M. Tajbakhsh, M. Chaudhry, Sources and controls of Arsenic contamination in groundwater of Rajnandgaon and Kanker District, Chattisgarh Central India, Journal of Hydrology, 395, 1-2, 2010, 49-66.
7. V.P. Dheeraj, A.K Sonkar, C.S. Singh, Evaluation of groundwater quality using water quality index (WQI) in Ambedkar Nagar City, Uttar Pradesh, India, In Recent Advancements in Civil Engineering: Select Proceedings of ACE, 2020, 429-441.
8. M.W. Aktar, M. Paramasivam, M. Ganguly, S. Purkait, D. Sengupta, Assessment and occurrence of various heavy metals in surface water of Ganga river around Kolkata: a study for toxicity and ecological impact, Environmental monitoring and assessment, 160, 2010, 207-213.
9. S. Selvam, S. Venkatramanan, C. Singaraja, A GIS-based assessment of water quality pollution indices for heavy metal contamination in Tuticorin Corporation, Tamilnadu, India, Arabian Journal of Geosciences, 8, 2015, 10611-10623.
10. K. Atkovska, K. Lisichkov, G. Ruseska, A.T. Dimitrov, A. Grozdanov, Removal of heavy metal ions from wastewater using conventional and nanosorbents: a rview, J. Chem. Technol. Metall., 53, 2, 2018, 202-217.

11. Z. Usmani, V. Kumar, Characterization, partitioning, and potential ecological risk quantification of trace elements in coal fly ash, Environmental Science and Pollution Research, 24, 2017, 15547-15566.
12. C. Brandon, K. Hommann, The cost of inaction: valuing the economy-wide cost of environmental degration in India, UNU, Institute of Advanced Studies, 1996.
13. G. Singh, R.K. Kamal, Heavy metal contamination and its indexing approach for groundwater of Goa mining region, India, Applied water science, 7, 2017, 1479-1485.
14. C.S. Lee, X.D. Li, G. Zhang, J. Li, A.J. Ding, T. Wang, Heavy metals and Pb isotopic composition of aerosols in urban and suburban areas of Hong Kong and Guangzhou, South China-evidence of the long-range transport of air contaminants, Atmospheric Environment, 41, 2, 2007, 432-447.
15. M.B. Lohani, A. Singh, D.C. Rupainwar, D.N. Dhar, Seasonal variations of heavy metal contamination in river Gomti of Lucknow city region, Environmental Monitoring and Assessment, 147, 2008, 253-263.
16. M.A. Aitouche, M. Djeddi, K. Baddari, Fractal variogram-based time - space of aftershock sequences analysis-case study: the May 21, 2003 Boumerdes-Algeria earthquake, Arabian Journal of Geosciences, 6, 2013, 2183-2192.
17. Geological survey of India, Data sharing and accessibility policy, 2019.
18. Geological survey of India, Final report on regional exploration for coal in the Bhelai East Area, South Central Part of Korba Coalfield, Bilaspur District, M.P., India, 1993.
19. R. Singh, A.S. Venkatesh, T.H. Syed, L. Surinaidu, S. Pasupuleti, S.P. Rai, M. Kumar, Stable isotope systematics and geochemical signatures constraining groundwater hydraulics in the mining environment of the Korba Coalfield, Central India, Environmental Earth Sciences, 77, 2018, 1-17.
20. A.K. Krishna, K.R. Mohan, N.N. Murthy, P.K Govil, Comparative study of X-ray fluorescence and inductively coupled plasma optical emission spectrometry of heavy metals in the analysis of soil samples, Spectrosc., 29, 3, 2008, 83-89.
21. WHO, Guidelines for drinking-water quality, World Health Organization, Geneva, 2006.
22. BIS, Indian standard drinking water-specification, second revision, Bureau of Indian Standards, New Delhi, 2012, 10500.
23. B. Prasad, J. Bose, Evaluation of the heavy metal pollution index for surface and spring water near a limestone mining area of the lower Himalayas, Environmental Geology, 41, 1, 2001, 183-188.
24. A.E. Edet, O.E. Offiong, Evaluation of water quality pollution indices for heavy metal contamination monitoring, A study case from Akpabuyo-Odukpani area, Lower Cross River Basin (Southeastern Nigeria), GeoJournal, 57, 2002, 295-304.
25. M.V. Prasanna, R. Nagarajan, S. Chidambaram, A. Elayaraja, Assessment of metals distribution and microbial contamination at selected Lake waters in and around Miri city, East Malaysia, Bulletin of Environmental Contamination and Toxicology, 89, 2012, 507-511.
26. B. Backman, D. Bodiš, P. Lahermo, S. Rapant, T. Tarvainen, Application of a groundwater contamination index in Finland and Slovakia, Environmental geology, 36, 1998, 55-64.
27. K.P. Singh, A. Malik, D. Mohan, S. Sinha, Multivariate statistical techniques for the evaluation of spatial and temporal variations in water quality of Gomti River (India)-a case study, Water research, 38, 18, 2004, 3980-3992.
28. A.M. Hassan, A.F. Ersoy, N.A. Turan, Assessment of heavy metal (loid) s in groundwater by multivariate statistical analysis and metals pollution indices: a case study of Çarşamba coastal aquifer, North Turkey, Arabian Journal of Geosciences, 14, 2021, 1-21.
29. R. Singh, A.S. Venkatesh, T.H. Syed, A.G.S. Reddy, M. Kumar, R.M. Kurakalva, Assessment of potentially toxic trace elements contamination in groundwater resources of the coal mining area of the Korba Coalfield, Central India, Environmental Earth Sciences, 76, 2017, 1-17.
30. L. Yu, G. Xin, W. Gang, Q. Zhang, S. Qiong, X. Guoju, Heavy metal contamination and source in arid agricultural soil in central Gansu Province, China, Journal of Environmental Sciences, 20, 5, 2008, 607-612.
31. S. Dragović, N. Mihailović, B. Gajić, Heavy metals in soils: distribution, relationship with soil characteristics and radionuclides and multivariate assessment of contamination sources, Chemosphere,

72, 3, 2008, 491-495.
32. D. Alexakis, Diagnosis of stream sediment quality and assessment of toxic element contamination sources in East Attica, Greece, Environmental Earth Sciences, 63, 2011, 1369-1383.
33. S.K. Reza, U. Baruah, S.K. Singh, T.H. Das, Geostatistical and multivariate analysis of soil heavy metal contamination near coal mining area, Northeastern India, Environmental Earth Sciences, 73, 2015, 5425-5433.
34. G. Stamatis, D. Alexakis, D. Gamvroula, G. Migiros, Groundwater quality assessment in Oropos-Kalamos basin, Attica, Greece, Environmental Earth Sciences, 64, 2011, 973-988.